

CT-based differentiation of solid pseudopapillary neoplasm and nonfunctional neuroendocrine tumor of pancreas

Yanqing Ma 

Yang Wen 

Jianguo Zhong 

PURPOSE

The purpose of this paper was to distinguish solid pseudopapillary neoplasms (SPNs) and nonfunctional neuroendocrine tumors (nf-NETs) of pancreas using univariate analysis and clinical-CT logistic regression model.

METHODS

Twenty-eight patients with SPNs and 46 patients with nf-NETs underwent enhanced CT examinations. Clinical data (sex, age), categorical (location, cystic degeneration, calcification, hemorrhage, and enhancement pattern), and numeric CT features (lesion long diameter, long/short diameter ratio, tumor attenuation values and tumor/pancreas attenuation ratios at unenhanced phase [UP], arterial phase [AP], and venous phase [VP]) were recorded. The logistic regression model was constructed by stepwise forward method of binary logistic regression after univariate analysis. The corresponding operating characteristic curve (ROC) and nomogram were delineated. The area under the curve (AUC), sensitivity, and specificity of ROC were calculated.

RESULTS

The SPNs were observed more often in relatively young ($P < .001$), female ($P < .001$) patients. After the univariate analysis, the categorical CT features of location ($P = .048$), hemorrhage ($P = .003$), and enhancement pattern ($P = .004$) and the numeric CT features of lesion long diameter ($P = .005$), tumor/pancreas_{UP} ($P = .002$), tumor_{AP} ($P < .001$), and tumor/pancreas_{AP} ($P < .001$) had statistical significance. The AUC (95% CI), sensitivity, and specificity of a logistic regression model composed of age, tumor/pancreas_{UP}, and tumor/pancreas_{AP} were 0.933 (95% CI, 0.850-0.978), 84.78%, and 92.86%.

CONCLUSION

The SPNs often occurred in 20- to 40-year-old female patients, were located in the body or tail of pancreas, showed hemorrhagic degeneration, heterogeneous enhancement, and were relatively larger in size compared with nf-NETs. Tumor/pancreas_{UP}, tumor_{AP}, and tumor/pancreas_{AP} values of SPNs were smaller than those of nf-NETs. The clinical-CT logistic regression model and nomogram consisting of age, tumor/pancreas_{UP}, and tumor/pancreas_{AP} parameters helped to differentiate SPNs from nf-NETs.

Solid pseudopapillary neoplasm (SPN) of pancreas is an uncommon and unique entity accounting for 1%-3% of all pancreatic tumors,¹ which was initially reported by Frantz in 1959² and designated as SPN by the World Health Organization (WHO) in 1996.³ According to the latest WHO classification of digestive tumors,⁴ SPN presents a low malignant potential and excellent long-term prognosis following surgical resection. Pancreatic neuroendocrine tumor (NET) is a neoplasm derived from progenitor islet cells⁵ and has been divided into functional NET (f-NET) and non-functional NET (nf-NET) based on their clinical symptoms caused by different hormones⁶ and the hormone levels detected by blood tests.

SPNs have various pathological and radiological features that overlap with other pancreatic neoplasms, in particular, nf-NETs. Microscopically, both SPNs and NETs comprise a monotonous and solid cell nest.⁷ Similar pseudopapillary-like cellular arrangement and expression of CD56 and synaptophysin further complicate the differentiation, while the diffused nuclear expression of β -captein is of great significance for the diagnosis of SPNs.⁷ Typically, most SPNs of the pancreas are

From the Department of Radiology (Y.M.

✉ 704180026@qq.com, Y.W., J.Z.), Zhejiang Provincial People's Hospital, People's Hospital of Hangzhou Medical College, Hangzhou, People's Republic of China.

Received 4 November 2020; revision requested 1 December 2020; last revision received 18 January 2020; accepted 26 January 2021.

DOI: 10.5152/dir.2022.20926

You may cite this article as: Ma Y, Wen Y, Zhong J. CT-based differentiation of solid pseudopapillary neoplasm and nonfunctional neuroendocrine tumor of pancreas. *Diagn Interv Radiol.* 2022;28(2):124-130.

large, well-encapsulated, and heterogeneous masses with areas of hemorrhagic, cystic, or calcific degeneration⁷ on computed tomography (CT) or magnetic resonance imaging (MRI). However, nf-NETs have a number of atypical characteristics, mimicking the presentation of SPNs on CT or MRI images. Thus, nf-NETs should be at the top of the differential diagnosis list. SPNs have a significantly better prognosis and survival compared to nf-NETs. Therefore, the distinction between them is of paramount importance.

To the best of our knowledge, few categorical and numeric CT logistic regression analyses have been reported to differentiate SPNs from nf-NETs. This retrospective study attempted to construct a clinical-CT logistic regression model to better distinguish these two diseases by systematic CT analysis.

Methods

This retrospective study was approved by our institutional review board (No. 2020 QT338) and the formal written consent was waived.

Patients

We reviewed all the pancreatic data at the picture archiving and communication system (PACS) from January 2013 to September 2020. The inclusion criteria were as follows: (a) all the patients were pathologically proven to have either SPNs or nf-NETs after surgical resections, (b) patients underwent enhanced CT examinations with the same scan protocol, (c) patients received preoperative CT examinations within 3 months before surgeries, and (d) the nf-NET patients did not have clinical symptoms caused by secreted hormones and had

normal hormone levels after blood tests. The exclusion criteria were as follows: (a) patients got radiation or chemotherapy treatment before CT examinations; (b) the quality of CT images were not good enough for analysis because of motion or breathe artifacts, parts of images lost, and so on; and (c) patients accompanied by other pancreatic diseases, such as inflammation or tumor. The specific workflow of patient recruitment was shown in Figure 1.

CT examinations

All three-phase enhanced CT scans were performed using a 64/128-multidetector CT (SOMATOM Definition AS, Siemens Healthcare). The three phases of CT examination consisted of unenhanced phase (UP), arterial phase (AP), and venous

phase (VP). Using the method of computer-aided bolus tracking technology and setting a 100 HU in the abdominal aorta as the threshold baseline, the AP and VP scans were performed with approximately 30 s and 60 s delay after administration of 90-100 mL nonionic contrast material (Iopromide, 370) via an antecubital vein at a rate of 3.0 mL/s. The tube voltage was 120 kVp and the tube current was 200 mA. The collimation was 64 × 0.625 mm and rotation time was 0.75 s. The slice thickness and intervals of images were both 5.0 mm.

CT image analysis

The CT image analysis included categorical and numeric assessments. Two radiologists (7 years and 10 years experience in abdominal diagnosis) worked together to

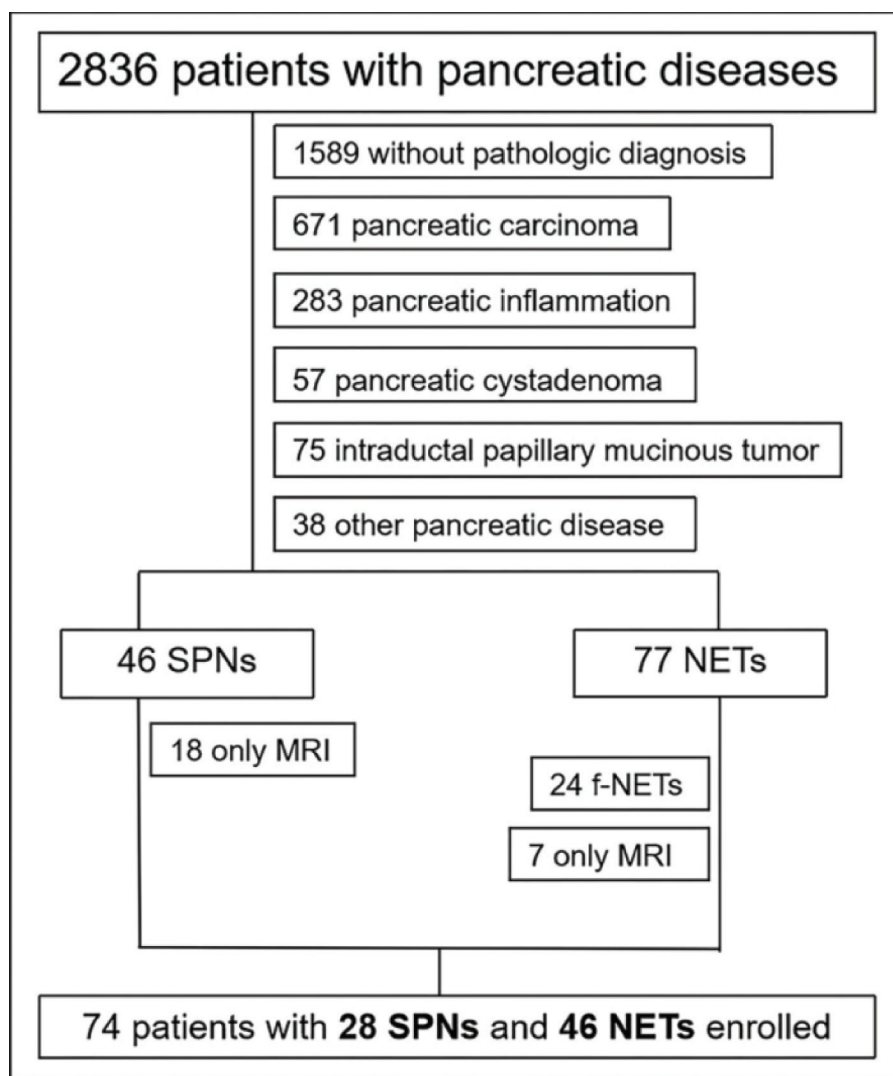


Figure 1. The workflow of patient selection. The other pancreatic diseases included accessory spleen, lymphoma infiltration, metastasis, simple cyst, and others. SPN, solid pseudopapillary neoplasm; NET, neuroendocrine tumor; f-NET, functional NET; MRI, magnetic resonance imaging.

Main points

- The solid pseudopapillary neoplasms (SPNs) often occurred in 20- to 40-year-old female patients, were located in the body or tail of pancreas, and showed hemorrhagic degeneration and heterogeneous enhancement compared with nonfunctional neuroendocrine tumors (nf-NETs).
- Tumor/pancreas_{UP}, tumor_{AP}, and tumor/pancreas_{AP} values of SPNs were smaller than those of nf-NETs.
- The most significant risk factors were age, tumor/pancreas_{UP}, and tumor/pancreas_{AP} in clinical-CT logistic regression model and nomogram which achieved promising discrimination between SPNs and nf-NETs.

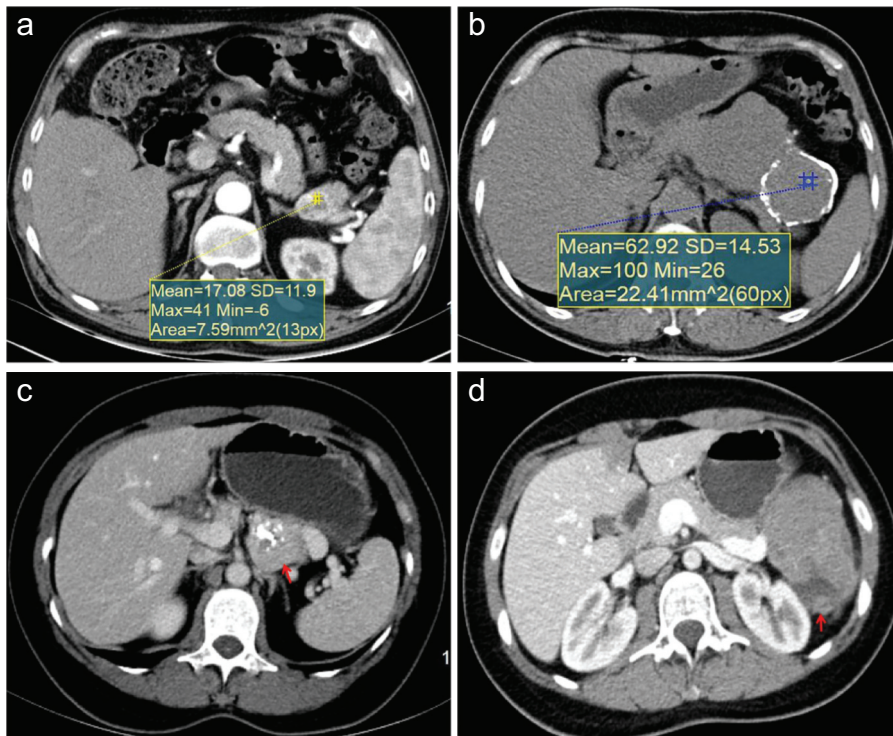


Figure 2. a-d. Axial arterial phase (AP) image (a) of a 60-year-old male with nf-NET in pancreatic tail shows the area of cystic degeneration. Axial unenhanced phase (UP) image (b) of a 45-year-old female with SPNs shows peripheral calcification and hemorrhage in the middle of lesion. Axial venous phase (VP) image (c) of a 50-year-old female with nf-NET displays calcification in the lesion and homogeneous enhancement of the solid component. Axial AP image (d) of a 21-year-old female with SPN, shows cystic degeneration and mildly heterogeneous enhancement in the mass.

analyze categorical CT images in consensus and blinded to the pathological results. The categorical features included location (head, body, or tail of pancreas), cystic degeneration (defined as the area with CT attenuation between that of fluid and soft tissue⁸ (Figure 2a, 2d), calcification (Figure 2b, 2c), hemorrhage defined according to the high-attenuation component greater than 45 Hu presented in the lesion⁹ (Figure 2b) and enhancement pattern categorized as homogeneous, mildly heterogeneous, and markedly heterogeneous by visual evaluation¹⁰ (Figure 2c, 2d).

The numeric characteristics were measured by two radiologists, respectively, and the mean values were taken for further analysis. The intraclass correlation coefficient (ICC) was calculated to assess the agreement between two radiologists. The regions of interest (ROIs) of tumor and pancreas were measured in the longer axis of the lesion and included the solid component of the lesion as much as possible.¹¹ The numeric characteristics were as follows: long diameter of the lesion, long-to-short diameter ratio (long/short diameter ratio), tumor CT attenuation on UP (tumor_{UP}), tumor-to-pancreas CT attenuation ratio on UP (tumor/pancreas_{UP}),

Table 1. The clinical data and CT characteristics of patients

	SPNs (n = 28)	nf-NETs (n = 46)	P
Clinical data			
Sex (female/male)	24 (85.7%)/4 (14.3%)	16 (34.8%)/30 (65.2%)	<.001
Age (mean ± standard)	34.14 ± 13.47	53.80 ± 13.23	<.001
Categorical analysis			
Location (head/body/tail)	6 (21.4%)/11 (39.3%)/11 (39.3%)	21 (45.7%)/8 (17.4%)/17 (36.9%)	.048
Cystic generation	14 (50.0%)	19 (41.3%)	.465
Calcification	7 (25.0%)	5 (10.9%)	.203
Hemorrhage	5 (17.9%)	0	.003
Enhancement pattern (homogeneous/mildly/markedly heterogeneous)	4 (14.3%)/10 (35.7%)/14 (50.0%)	23 (50.0%)/6 (13.0%)/17 (37.0%)	.004
Numeric analysis			
Lesion long diameter (mm)	45.50 (21.00-156.00)	33.50 (6.00-132.00)	.005*
Long/short diameter ratio	0.85 ± 0.10	0.80 ± 0.12	.055
Tumor _{UP} (HU)	35.71 ± 7.17	37.06 ± 7.58	.451
Tumor/pancreas _{UP}	0.72 (0.47-1.12)	0.86 (0.50-1.95)	.002*
Tumor _{AP} (HU)	22.63 ± 12.29	61.21 ± 43.98	<.001
Tumor/pancreas _{AP}	0.20 ± 0.10	0.65 ± 0.44	<.001
Tumor _{VP} (HU)	7.90 (-16.50 to 20.30)	1.05 (-68.30 to 57.30)	.152*
Tumor/pancreas _{VP}	0.09 (-0.17 to 0.21)	0.01 (-0.73 to 0.54)	.155*

SPNs, solid pseudopapillary neoplasms; nf-NETs, nonfunctional neuroendocrine tumors; HU, Hounsfield units; UP, unenhanced phase; AP, arterial phase; VP, venous phase.

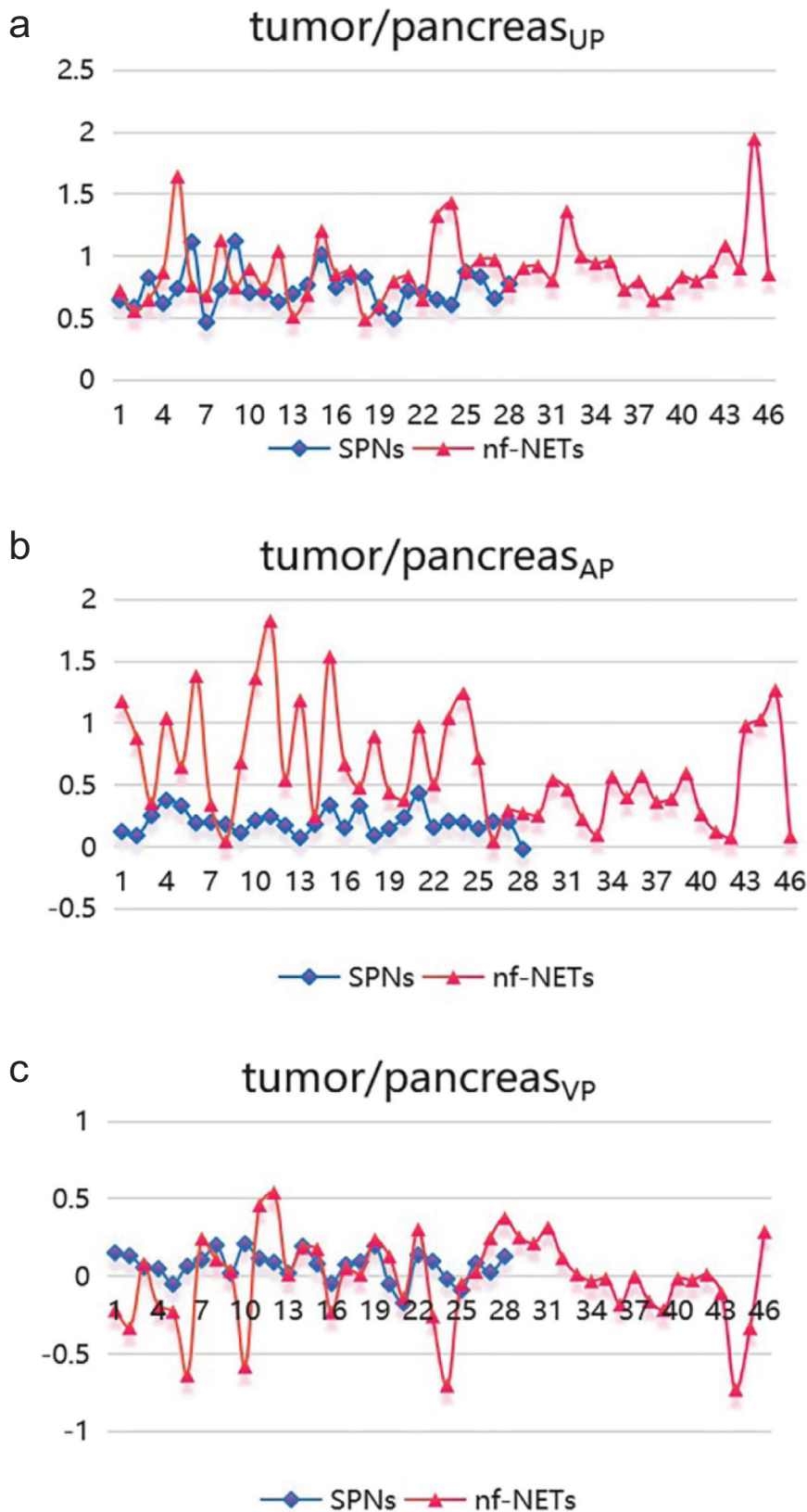


Figure 3. a-c. The tumor/pancreas_{UP} and tumor/pancreas_{AP} of SPNs were significantly smaller than those of nf-NETs. However, the tumor/pancreas_{VP} had no statistical difference between two diseases.

tumor-enhanced CT attenuation on AP (tumor_{AP'} calculated as the difference value of tumor CT attenuation between the AP and UP), tumor-to-pancreas CT attenuation ratio on AP (tumor/pancreas_{AP}), tumor-enhanced CT attenuation on VP (tumor_{VP'} calculated as the difference value of tumor CT attenuation between the VP and AP), and tumor-to-pancreas CT attenuation ratio on VP (tumor/pancreas_{VP}).

Statistical analysis

The analysis of categorical CT features was analyzed using Pearson chi-square test or Fisher exact probabilities method. The analysis of numeric CT features was analyzed by method of independent-sample t test or Mann-Whitney *U*-test if variables distributed non-normally. The skewness and kurtosis values were calculated to test the normality of numeric variables. The normal distributed variables were described as average \pm standard deviation, while the non-normal distributed ones were described as median (min-max) values. Then, the significant risk factors were enrolled to construct logistic regression model by the method of stepwise forward binary logistic regression. The Hosmer-Lemeshow test was made to evaluate the fitting degree of the logistic regression model. These statistical methods were performed using IBM SPSS Statistics (Version 22.0). The ICC of numeric CT features between two radiologists and the ROC of corresponding logistic regression model were made on software of MedCalc (Version 18.2.1). The relative nomogram was depicted using R software (Version 4.1.0). A two-tailed $P < .05$ was considered statistically significant. The P value $> .05$ of Hosmer-Lemeshow test indicated the goodness of fit. The ICC > 0.75 suggested good consistency between different observers.

Results

Results of clinical data and CT characteristics were summarized in Table 1. Typically, SPNs occurred more frequently in female ($P < .001$) and younger patients than nf-NETs (34.14 ± 13.47 vs. 53.80 ± 13.23 , $P < .001$).

In categorical CT analysis, cystic generation and calcification showed no statistical significance between SPNs and nf-NETs. Meanwhile, hemorrhagic ($P = .003$), heterogeneously enhanced ($P = .004$) masses in

Table 2. The result of logistic regression model

	B	S.E.	Wald	P	Exp (B)	95%EXP(B)
Age	0.082	0.029	7.877	.005	1.085	1.025-1.149
Tumor/pancreas _{UP}	5.809	2.736	4.509	.034	333.371	1.564-71,046.093
Tumor/pancreas _{AP}	9.146	3.149	8.436	.004	9380.606	19.575-44,953,596.969
Constant	-10.232	3.017	11.498	.001	0.000	

S.E., standard error; UP, unenhanced phase; AP, arterial phase.

body or tail ($P = .048$) of pancreas tended to be diagnosed as SPNs.

In numeric analysis, the ICC between radiologists was 0.782-0.895, which indicated good agreement ($ICC > 0.75$) between two radiologists. The long diameter ($P = .005$) of the SPN was generally longer than that of the nf-NET (average \pm standard deviation, 55.39 ± 29.46 mm vs. 37.20 ± 22.98 mm). However, the long/short diameter ratio showed no significant difference between the two diseases. Compared with nf-NETs, the values of tumor/pancreas_{UP} ($P = .002$, Figure 3a), tumor_{AP} ($P < .001$), and tumor/pancreas_{AP} ($P < .001$, Figure 3b) of SPNs were relatively smaller. On the other hand, the tumor_{UP}, tumor_{VP}, and tumor/pancreas_{VP} (Figure 3c) were not statistically different between SPNs and nf-NETs.

Significant risk factors of sex, age, location, hemorrhage, enhancement pattern, lesion long diameter, tumor/pancreas_{UP}, tumor_{AP}, and tumor/pancreas_{AP} were included in the logistic regression analysis. Finally, the clinical-CT logistic regression model (Table 2) was constructed based on three independent predictors of age ($P = .005$), tumor/pancreas_{UP} ($P = .034$), and tumor/pancreas_{AP} ($P = .004$). The non-significant Hosmer-Lemeshow ($P = .674$) showed suggested goodness of fit of this logistic regression model. The equation of the model was: $Y = -10.232 + 0.082 * [\text{age}] + 5.809 * [\text{tumor/pancreas}_{UP}] + 9.146 * [\text{tumor/pancreas}_{AP}]$. Then, the ROC (Figure 4) and nomogram (Figure 5) were delineated according to this logistic regression model. The AUC (95% CI), sensitivity, and specificity of ROC in distinguishing SPNs and nf-NETs were 0.933 (95% CI, 0.850-0.978), 84.78%, and 92.86%.

Discussion

To date, only a few publications compared the imaging features between SPNs and NETs using univariate analysis,¹² and there has been no CT-based logistic

differentiation of SPNs and nf-NETs. Among the 28 SPNs patients enrolled in this study, 7 patients (25.0%) were misdiagnosed as nf-NETs. Meanwhile, 14 out of 46 nf-NETs patients were misdiagnosed, of which 6 (13.0%) were misdiagnosed as SPNs. Thus, the distinction between SPNs and nf-NETs is clinically important. The first section of this study focused on the univariate analysis of clinical and CT features. The SPNs usually showed the following categorical features: female predominance (85.7%), younger age (34.14 ± 13.47 years vs. 53.8 ± 13.23 years), location in pancreatic body or tail (78.6%), hemorrhage (17.9%), and heterogeneous enhancement

(85.7%). There is a consensus that SPNs tend to occur in young female patients.^{13,14} Data from previous studies have suggested that SPNs often located in the body or tail of pancreas,¹⁵ also consistent with our result. Ventriglia et al.¹⁶ highlighted that specific MRI features of internal hemorrhage and well demarcation helped to differentiate SPNs from other cystic pancreatic tumors. Intratumoral hemorrhage must be considered as an important pathological characteristics of SPNs¹⁷ even if it was just found in 5/28 (17.9%) in this study. It has been demonstrated that the presence of cystic pattern or hemorrhage in varying proportions are the results of

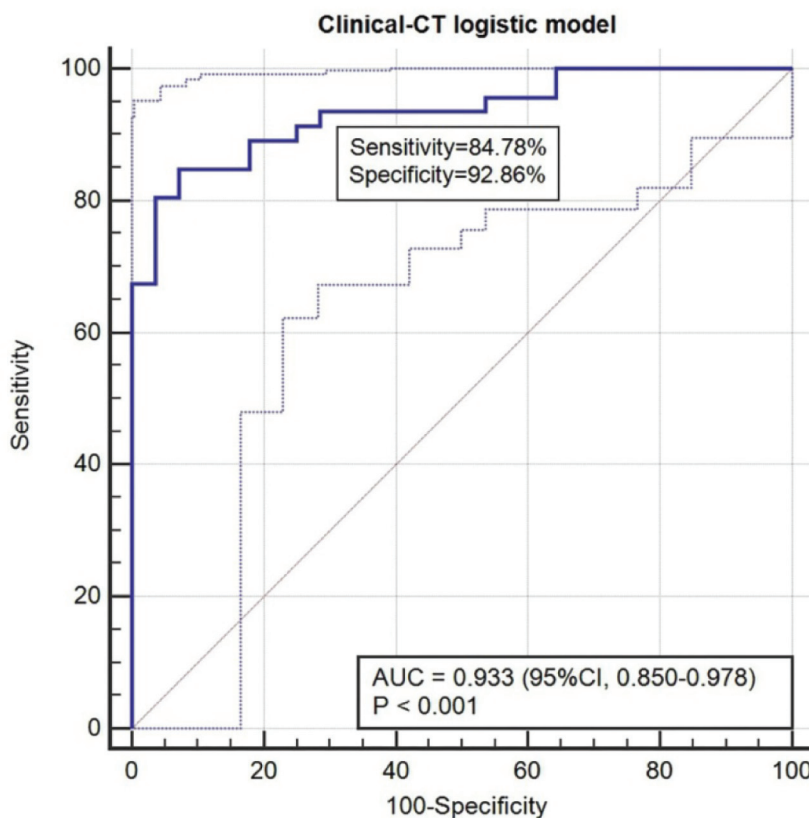


Figure 4. The ROC curve of clinical-CT logistic regression model in differentiating SPNs from nf-NETs.

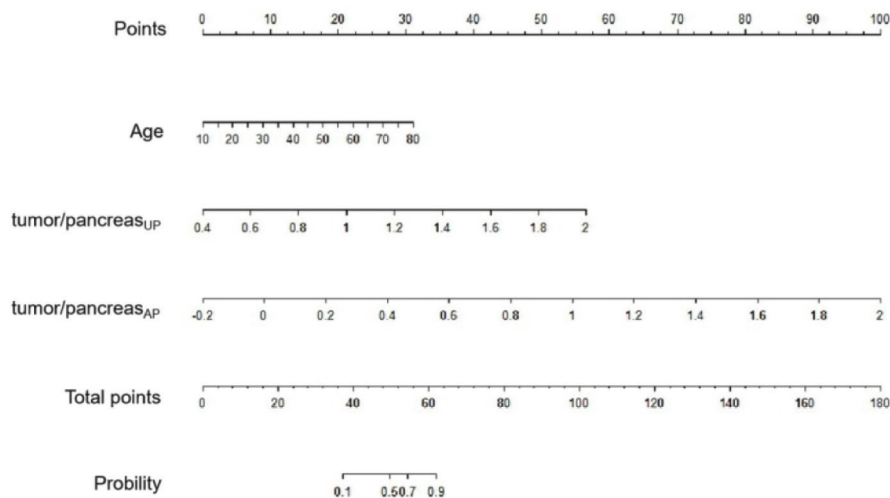


Figure 5. The nomogram to diagnose nf-NETs after differentiating from SPNs based on clinical-CT logistic regression. UP, unenhanced phase; AP, arterial phase.

a process of degeneration.¹⁸ However, no statistical difference was noted in features of cystic degeneration and calcification between SPNs and nf-NETs in our study. Heterogeneous enhancement corresponded with tumoral degeneration, which has been histopathologically proved.¹⁹

A previous publication assessing the enhancement manifestation by visual evaluation of MRI illustrated that all SPNs had early heterogeneous and progressive enhancement pattern, but 67% of NETs showed persistent homogeneous enhancement.²⁰ This paper gave a detailed measurement of CT attenuation and found that smaller tumor/pancreas_{UP}, tumor/pancreas_{AP}, and tumor/pancreas_{VP} were associated with SPNs. The relative CT attenuation of tumor/pancreas_{UP}, tumor/pancreas_{AP}, and tumor/pancreas_{VP} were calculated after standardization against pancreas, reducing the inter-individual variability. Regarding the VP of CT examination, SPNs had similar enhancement with nf-NETs in this analysis, which was not tally with previous results.²¹

After the univariate analysis of clinical data and CT features, a logistic regression model was built, achieving a promising performance in differentiating SPNs from nf-NETs. The AUC of this model was 0.933. This clinical-CT logistic regression model included age, tumor/pancreas_{UP}, and tumor/pancreas_{AP}. Compared with CT attenuation, the relative attenuation of tumor/pancreas_{UP} and tumor/pancreas_{AP} played an important role in differentiating SPNs from nf-NETs, while

the VP enhancement did not help to diagnose the diseases significantly, although previous studies had reported that nf-NETs presented a rapid and homogeneous enhancement in MRI images.²¹ This result presumably related to the delay time in VP, though there is no standard scan protocol. The corresponding nomogram achieved straightforward and visualized noninvasive distinction between the SPNs and nf-NETs. This information presented integrated clinical data and CT characteristics and provided a scoring system to facilitate differential diagnosis between two diseases.

There were some limitations in our study. First, the sample size was small because of the rarity of tumors. Moreover, this small sample size restricted the study in morphology of calcification, and different grades of nf-NETs. Second, the characteristics of a tumor capsule of the SPN and floating cloud sign were not analyzed in this paper which need further analysis. Previous studies confirmed that the well-defined capsule facilitated the diagnosis of SPN in MRI images²⁰ and proved focally defective capsule histopathologically.⁷ Third, this retrospective study only differentiated SPNs from nf-NETs because of considerable overlap in CT images. Nevertheless, other pancreatic lesions, such as carcinoma or cystadenoma of pancreas also need future analysis. Fourth, on the numeric analysis of CT attenuation, only the solid portion of the mass was measured and the regions of cystic degeneration, calcification, and hemorrhage were ignored.

In conclusion, the SPNs often occurred in 20- to 40-year-old female patients, were located in the body or tail of pancreas, showed hemorrhagic degeneration and heterogeneous enhancement, and were relatively larger compared with nf-NETs. The clinical-CT logistic regression model and nomogram including age, tumor/pancreas_{UP}, and tumor/pancreas_{AP} achieved promising discrimination between SPNs and nf-NETs.

Conflict of interest disclosure

The authors declared no conflicts of interest.

References

- Papavramidis T, Papavramidis S. Solid pseudopapillary tumors of the pancreas: Review of 718 patients reported in English literature. *J Am Coll Surg.* 2005;200(6):965-972. [Crossref]
- Franz V. *Papillary Tumors of the Pancreas: Benign or Malignant.* US Armed Forces Institute of Pathology Atlas of tumor pathology Washington DC.1959.
- Hopwood. Histological typing of tumours of the exocrine pancreas. *J Clin Pathol.* 1996;49(9):780. [Crossref]
- Nagtegaal ID, Odze RD, Klimstra D, et al. The 2019 WHO classification of tumours of the digestive system. *Histopathology.* 2020;76(2):182-188. [Crossref]
- Rindi G, Wiedenmann B. Neuroendocrine neoplasms of the gut and pancreas: New insights. *Nat Rev Endocrinol.* 2012;8(1):54-64. [Crossref]
- Eckhauser FE, Cheung PS, Vinik AI, Strodel WE, Lloyd RV, Thompson NW. Nonfunctioning malignant neuroendocrine tumors of the pancreas. *Surgery.* 1986;100:978-988.
- Notohara K, Wani Y, Fujisawa M. Solid pseudopapillary neoplasm: Pathological diagnosis and distinction from other solid cellular tumours of the pancreas. *Diagn Histopathol.* 2008;14:266-274. [Crossref]
- Buetow PC, Buck JL, Pantongrag-Brown L, Beck KG, Ros PR, Adair CF. Solid and papillary epithelial neoplasm of the pancreas: Imaging-pathologic correlation on 56 cases. *Radiology.* 1996;199(3):707-711. [Crossref]
- Rastogi A, Assing M, Taggart M, et al. Does Computed Tomography Have the Ability to Differentiate Aggressive From Nonaggressive Solid Pseudopapillary Neoplasm? *J Comput Assist Tomogr.* 2017;42(3):405-411. [Crossref]
- Takahashi N, Leng S, Kitajima K, et al. Small (< 4 cm) renal masses: Differentiation of angio-myolipoma without visible fat from renal cell carcinoma using unenhanced and contrast-enhanced CT. *AJR Am J Roentgenol.* 2015;205:1194-1202. [Crossref]
- Li J, Lu J, Liang P, et al. Differentiation of atypical pancreatic neuroendocrine tumors from pancreatic ductal adenocarcinomas: Using whole-tumor CT texture analysis as quantitative biomarkers. *Cancer Med.* 2018;7(10):4924-4931. [Crossref]

12. Yu MH, Lee Jy Fau Kim MA, Kim Ma Fau Kim SH, et al. MR imaging features of small solid pseudopapillary tumors: Retrospective differentiation from other small solid pancreatic tumors. *AJR Am J Roentgenol.* 2010;195(6):1324-1332. [\[Crossref\]](#)
13. Young Keun Sur JHL, Jai Keun K, Min Jung P. Comparison of MR imaging features of solid pseudopapillary neoplasm of pancreas between male and female patients. *Eur J Radiol.* 2015;84(11):2065-2070. [\[Crossref\]](#)
14. Peyman D, Jinping L. Solid pseudopapillary neoplasm of the pancreas: A rare entity with unique features. *Arch Pathol Lab Med.* 2017;141(7):990-995. [\[Crossref\]](#)
15. Nakache R, Nachmany I, Lubezky N, et al. Solid pseudopapillary neoplasm of the pancreas: Management and long-term outcome. *Eur J Surg Oncol.* 2017;43(6):1056-1060. [\[Crossref\]](#)
16. Ventriglia A, Manfredi R, Mehrabi S, et al. MRI features of solid pseudopapillary neoplasm of the pancreas. *Abd Imag.* 2014;39(6):1213-1220. [\[Crossref\]](#)
17. Klotz T, Ines DD, Petitcolin V, Lannareix V, Essamet W, Garcier JM. Solid pseudopapillary neoplasm of the pancreas. *Diagn Interven Imag.* 2015;29:93-96.
18. Kosmahl M, Seada LS, Jnig U, Harms D, Klppel G. Solid-pseudopapillary tumor of the pancreas: Its origin revisited. *Arch Pathol Anat Phys Klinische Med.* 2000;436(5):473-480.
19. Marchegiani G, Andrianello S, Massignani M, et al. Solid pseudopapillary tumors of the pancreas: Specific pathological features predict the likelihood of postoperative recurrence. *J Surg Oncol.* 2016;114(5):597-601. [\[Crossref\]](#)
20. Rai S, Prabhu S, Nirupama M, Adiga DS, Kumar A, Chakraborti S. Image findings of solid pseudopapillary neoplasms of the pancreas on multiphasic multidetector CT scan: A single institute experience from Southern India. *J Clin Diagn Res.* 2017;11(9):TC01–TC05.
21. Dong DJ, Zhang SZ. Solid-pseudopapillary tumor of the pancreas: CT and MRI features of 3 cases. *HBPD INT.* 2006;5(2):300-304.